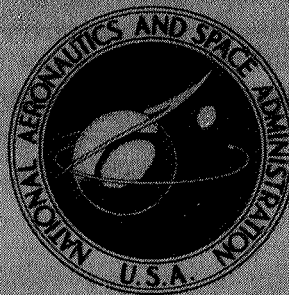


NASA TECHNICAL  
MEMORANDUM



NASA TM X-2643

NASA TM X-2643

AERODYNAMIC EFFECTS  
OF LEADING-EDGE SERRATIONS  
ON A TWO-DIMENSIONAL AIRFOIL

*by Paul T. Soderman*

*Ames Research Center*

*and*

*U.S. Army Air Mobility R&D Laboratory*

*Moffett Field, Calif. 94035*

NATIONAL AERONAUTICS AND SPACE ADMINISTRATION • WASHINGTON, D. C. • SEPTEMBER 1972

1. Report No. NASA TM X-2643	2. Government Accession No.	3. Recipient's Catalog No.	
4. Title and Subtitle <b>AERODYNAMIC EFFECTS OF LEADING-EDGE SERRATIONS ON A TWO-DIMENSIONAL AIRFOIL</b>		5. Report Date September 1972	
		6. Performing Organization Code	
7. Author(s) Paul T. Soderman		8. Performing Organization Report No. A-3706	
		10. Work Unit No. 136-13-01-08-00-21	
9. Performing Organization Name and Address NASA Ames Research Center and U.S. Army Air Mobility R&D Laboratory Moffett Field, Calif. 94035		11. Contract or Grant No.	
		13. Type of Report and Period Covered Technical Memorandum	
12. Sponsoring Agency Name and Address National Aeronautics and Space Administration Washington, D. C. 20545		14. Sponsoring Agency Code	
15. Supplementary Notes Edited by NASA Ames Research Center			
16. Abstract  An investigation was conducted to determine the flow field and aerodynamic effects of leading-edge serrations on a two-dimensional airfoil at a Mach number of 0.13. The model was an NACA 66 <sub>1</sub> -012 airfoil section with a 0.76 m (30 in.) chord, 1.02 m (40 in.) span, and floor and end plates. It was mounted in the Ames 7-by 10-Foot Wind Tunnel. Serrated brass strips of various sizes and shapes were attached to the model in the region of the leading edge. Force and moment data, and photographs of tuft patterns and of oil flow patterns are presented.  Results indicated that the smaller serrations, when properly placed on the airfoil, created vortices that increased maximum lift and angle of attack for maximum lift. The drag of the airfoil was not increased by these serrations at airfoil angles of attack near zero and was decreased at large angles of attack. Important parameters were serration size, position on the airfoil, and spacing between serrations.			
17. Key Words (Suggested by Author(s)) Leading-edge serration Vortex generator Flow separation Aerodynamic noise Maximum lift		18. Distribution Statement  Unclassified - Unlimited	
19. Security Classif. (of this report) Unclassified	20. Security Classif. (of this page) Unclassified	21. No. of Pages 38	22. Price* \$3.00

\* For sale by the National Technical Information Service, Springfield, Virginia 22151

## NOTATION

$C_L$	lift coefficient, $\frac{\text{lift}}{q_\infty S}$
$C_D$	drag coefficient, $\frac{\text{drag}}{q_\infty S}$
$C_m$	pitching-moment coefficient about 0.25 chord, $\frac{\text{pitching-moment}}{q_\infty S c}$
$S$	airfoil area, 0.774 m <sup>2</sup> (8.33 ft <sup>2</sup> )
$c$	airfoil chord, 0.76 m (2.5 ft)
$q_\infty$	free-stream dynamic pressure, N/m <sup>2</sup> (lb/sq ft)
$\alpha$	angle of attack of airfoil, deg
$R$	Reynolds number
$LE$	leading-edge serration

### Subscript

$u$  uncorrected

# AERODYNAMIC EFFECTS OF LEADING-EDGE SERRATIONS ON A TWO-DIMENSIONAL AIRFOIL

Paul T. Soderman

Ames Research Center  
and

U.S. Army Air Mobility Research and Development Laboratory

## SUMMARY

An investigation was conducted to determine the flow field and aerodynamic effects of leading-edge serrations on a two-dimensional airfoil at a Mach number of 0.13. The model was an NACA 66<sub>1</sub>-012 airfoil section with a 0.76 m (30 in.) chord, 1.02 m (40 in.) span, and floor and end plates. It was mounted in the Ames 7- by 10-Foot Wind Tunnel. Serrated brass strips of various sizes and shapes were attached to the model in the region of the leading edge. Force and moment data, and photographs of tuft patterns and of oil flow patterns are presented.

Results indicated that the smaller serrations, when properly placed on the airfoil, created vortices that increased maximum lift and angle of attack for maximum lift. The drag of the airfoil was not increased by these serrations at airfoil angles of attack near zero and was decreased at large angles of attack. Important parameters were serration size, position on the airfoil, and spacing between serrations.

## INTRODUCTION

The need to reduce the aerodynamic noise generated by gas turbine engines, rotors, and propellers has been well established. Investigations at Ames and elsewhere are being made on the effect of serrated leading edges on reducing noise generated by airfoils. Initial acoustic tests (refs. 1 and 2), showed that serrations reduce airfoil noise generation under certain conditions, but the flow mechanisms involved with the noise reduction have not been completely understood. Therefore, the aerodynamic effect of these serrations on a two-dimensional wind tunnel model was studied to determine the changes in flow field around the model. The results of this test are of general interest and may have applications not directly associated with noise reduction, such as delay of airfoil stall.

This report is the result of tests in the Ames 7- by 10-Foot Wind Tunnel of a two-dimensional airfoil with various leading-edge serrations. Serration size, shape, and location on the airfoil were varied. Lift, drag, and pitching moments were measured. Photographs of surface tufts showed separated flow patterns; photographs of oil flow showed surface streamline changes. Most data were taken at a dynamic pressure of 119.70 N/m<sup>2</sup> (25 lb/ft<sup>2</sup>) and a Reynolds number of  $2.32 \times 10^6$  based on the chord. Some data were taken at  $q_\infty = 239.4$  N/m<sup>2</sup> (5 lb/ft<sup>2</sup>) and  $R = 1.03 \times 10^6$ .

## MODEL AND APPARATUS

### Two-Dimensional Airfoil

An NACA 66<sub>1</sub>-012 wood airfoil with a steel spar was mounted in the floor of the 7- by 10-Foot Wind Tunnel. The airfoil had a 0.76 m (30 in.) chord and a 1.02 m (40 in.) span with floor and end plates fixed to the airfoil. Figure 1 shows the model mounted in the test section. The model rotated about its midchord line. Geometric details and dimensions are given in figure 2(a).

### Leading-Edge Serrations

The serrations were made from 0.0254 cm (0.010 in.) thick spring brass. Figure 2(b) shows the serration sizes and shapes and the numbers used to identify each one. The serrated strips were screwed to the airfoil lower surface with bases tangent to the surface (fig. 2(c) top). The locations of the attachment holes on the airfoil leading edge shown in figure 2(c) (bottom) correspond to the holes shown on the brass strips in figure 2(b). Figure 2(c) can be used to determine the exact location of any serration noted in the remaining figures. Photographs of some typical serrations mounted on the airfoil are presented in figure 2(d).

## CORRECTIONS

The wind tunnel data were corrected by removing the effects of end plates and support rods. These effects ( $\Delta C_D = -0.067$ ,  $\Delta C_m = 0.02$ ) were estimated by data from reference 3. In addition, the data were corrected for wind-tunnel wall effects (only the drag correction was significant). The total corrections were

$$\alpha = \alpha_u$$

$$C_D = C_{Du} - 0.067 + 0.015 C_{Lu}^2$$

$$C_L = C_{Lu}$$

$$C_m = C_{mu} + 0.02$$

## TESTING AND PROCEDURE

Wind-tunnel model forces and moments were measured in most cases through an angle of attack range of  $-2^\circ$  to  $+16^\circ$ . Pitching moments were computed about a moment center at the 25 percent chord. Leading-edge serration size, shape, and position were varied. Most tests were conducted at a Reynolds number of  $2.32 \times 10^6$  based on a 0.76 m chord and at a dynamic pressure of  $1197.0 \text{ N/m}^2$  ( $25 \text{ lb/ft}^2$ ).

All force and moment data presented were taken with two rows of tufts on the airfoil upper surface. The data labeled basic airfoil were taken with no serrations on the airfoil and with the leading-edge attachment holes faired smooth with red wax. A comparison of tufted and untufted model force data (not presented) showed that tufts increased  $C_D$ ,  $C_L$ , and  $C_m$  by 0.002, -0.02 and 0.006, respectively, through the angle-of-attack range.

## RESULTS

Figures 3 through 10 show the effects of serration size, geometry, location on the airfoil, and Reynolds number. Photographs of tufts on the model (figs. 11(a)-(f)) illustrate the effect of the serrations on the surface flow characteristics. Photographs of oil flow (figs. 12(a)-(c)), illustrate the vortices generated by the serrations.

## DISCUSSION

### Effect of Serration Size

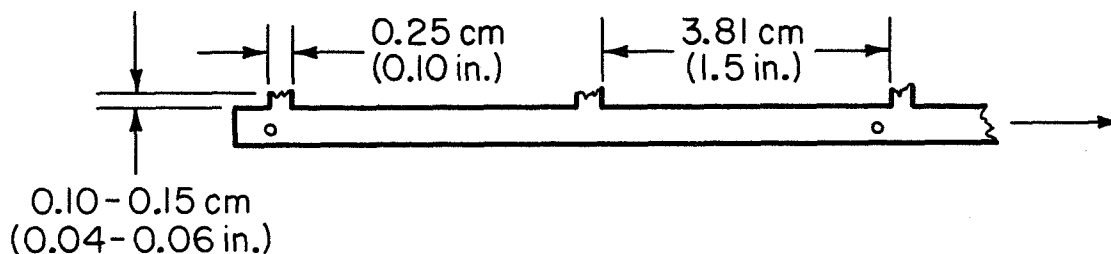
The size of the serrations was an important parameter in this experiment. The smaller serrations (0.51 cm (0.2 in.) and below) caused an increase in maximum lift and angle of attack for maximum lift by generating vortices that energized the boundary layer on the upper surface, as discussed in the section on Flow Studies. Figures 3, 4, and 5 illustrate the effect of serration size. Figure 3 shows that LE-8 and LE-10, which were smaller serrations (0.51 cm) increased maximum lift 12 percent but reduced the lift-curve slope. They were not the best serrations tested. The larger leading-edge serrations (LE-3 and LE-5) and the strip without serrations (LE-00) caused a reduction in maximum lift (figs. 4 and 5). These data agree generally with results obtained previously for airfoils with protuberances (ref. 4). Serrations that are too large, apparently obstruct the flow over the upper surface rather than perturb the flow as the small serrations do. The flow mechanisms are different. The minimum drag coefficients were not changed appreciably by the serrations since the serrations were placed near the stagnation point where the flow speed is low.

### Serration Geometry

Serration lean (spanwise cant angle) was another parameter investigated. Figure 3, which shows the results for LE-8 and LE-10, indicates that serration lean had very little effect on the results.

A comparison of serrations LE-7 (no gap) and LE-8 (0.25 cm (0.1 in.) gap) in figure 6 shows that some improvement in maximum lift was achieved by leaving a gap between the prongs. To explore this phenomenon further, some of the prongs in LE-8 were cut out in several stages to determine the effect of gap width on airfoil force data (modifications 1-4). These results (figs. 7(a) and (b)) indicate that increasing gap width from 0.25 to 0.75 cm (0.1 to 0.3 in.) did indeed increase maximum lift and lift-curve slope. Maximum lift, however, was relatively insensitive to further increases in gap width (i.e., 1.78 and 3.81 cm (0.7 and 1.5 in.)). Furthermore, LE-8,

modification 4, which was a serration with all the prongs cut down, as shown in the following sketch, increased maximum lift as much as the strip with complete prongs did. It is not known



LE-8, modification 4

whether the delay of airfoil stall by LE-8, modification 4, was due to vortex generation at the cut-down prongs or to a different phenomenon, namely, tripping of the laminar boundary layer all along the strip. A turbulent boundary layer would eliminate any separation bubble near the leading edge and change the airfoil stall. Flow visualization studies discussed in a following section showed that the full size prongs generated vortices. However, no flow studies were made to determine the size at which small protuberances near the airfoil leading edge become boundary-layer trips rather than vortex generators.

Curved serrations LE-A, B and C increased the maximum lift almost as much as did the uncurved serrations (see figs. 8(a)-(c)). However, curved serrations are more difficult to fabricate.

#### Serration Position

The position of the leading-edge serration on the airfoil lower surface was found to be the most critical parameter investigated. Figure 9 shows the results for LE-11 in positions 1, 2, 3, and 4 where position 1 corresponds to the chordline and position 4 corresponds to the most aft position tested. Of all configurations tested, LE-11 in position 4 caused the greatest increase in maximum lift ( $\Delta C_{L_{max}} = 0.21$ ). Position 4 was in the airfoil stagnation point region at angles of attack near stall. Notice that position 1 (zero percent chord), a serration location that caused a loss of lift and increase of drag, was only 0.95 cm (0.375 in.) from position 4 (1.25 percent chord), the best location. Serration positions aft of position 4 were not tested, but it is doubtful if serrations aft of the stagnation point could have affected stall on the upper surface.

#### Reynolds Number

The Reynolds number was reduced from  $2.32 \times 10^6$  to  $1.03 \times 10^6$  during part of the test. Reynolds numbers above  $2.32 \times 10^6$  could not be reached because of end-plate buffet. The results in figure 10 show that Reynolds number in the range studied had little effect on either the basic airfoil or the airfoil with serrations. The pitching-moment data are not presented because the curves overlap each other.

## Flow Studies

Tuft studies showed that the serrations delayed flow separation on the upper airfoil surface at various angles of attack (figs. 11(a)-(f)). The flow characteristics of the basic airfoil with two different sets of tufts are shown in figures 11(a) and (b). Note that the end plates did not maintain two-dimensional flow except near midspan. At stall the flow separated prematurely near the end plates. Consequently, the force data from this test cannot be compared directly with two-dimensional airfoil data for the 66<sub>1</sub>-012 section. In addition, what appears to be a leading-edge separation bubble in figure 11(a) may have been local separation induced by the end plate. Therefore, in general, the serrations will reduce separated flow on airfoils and will delay stall of airfoils with stall patterns like those of the model discussed here. The results of this study are not necessarily indicative of what might happen to an airfoil with different stall characteristics, nor will the effect of serrations on a truly two-dimensional 66<sub>1</sub>-012 airfoil necessarily be identical to those reported here.

The larger serration, LE-3, caused the model to stall sooner than did the unserrated model (fig. 11(c)). As mentioned before, the larger serrations probably obstructed the flow over the upper surface rather than perturbed the flow. LE-8, a smaller serration, had the opposite effect (fig. 11(d)). The leading-edge separation was eliminated and the trailing-edge separation was delayed to higher angles of attack than for the basic airfoil. Flow characteristics improved even more with LE-11 (fig. 11(e)).

The increased lift due to the serrations was caused by the generation of vortices that provided higher energy air to the boundary layer, delaying flow separation. The photographs of oil flow on the model<sup>1</sup> (figs. 12(a)-(c)) show the chordwise vortices on the upper surface trailing from serration LE-10 in position 3. Alternate white and dark bands were etched in the oil behind each prong from the airfoil leading edge to the trailing edge. The close-up photograph in figure 12(b) was taken before the chordwise bands were able to develop distinctly. However, the region near the leading edge shows the three-dimensional flow pattern created by the serrations. It appeared that counterrotating vortices from each prong formed a circular pattern aft of the serration and then trailed chordwise. However, the exact three-dimensional flow mechanism is not understood. The alternate dark and white bands are somewhat clearer on the left side (upper surface) of figure 12(c). The oil on the lower surface was applied near the leading edge and trailed aft in streaks (fig. 12(c)). The counterrotating vortex pairs on the upper surface appeared to be much like the Görtler type vortices formed behind a rearward facing step (ref. 5). It is possible that the flow conditions near the airfoil leading edge were similar to flow near the stagnation point on a flat wall, which can produce Görtler type vortices with a range of wave lengths (see ref. 6). Therefore, the serrations may amplify these vortices of a preferred wave length corresponding to the prong spacing.

## CONCLUDING REMARKS

The leading-edge serrations were effective in reducing separated flow on the model. However, the results are not directly applicable to two-dimensional airfoils since the end plates did not

---

<sup>1</sup>A mixture of titanium dioxide and vacuum pump oil.

maintain two-dimensional flow over the model. Separated flow progressed inboard from the end plates with increased angle of attack. The serrations delayed the onset of separated flow to higher angles of attack and increased maximum lift and angle of attack for maximum lift of the model.

The smaller serrations (0.10 to 0.50 cm (0.04 to 0.20 in.)) attached to the airfoil leading edge 0.95 cm (0.375 in.) from the chordline on the lower surface were most effective in reducing separation. This was deduced from the fact that the maximum lift was greatest for those serrations. The drag at low angles of attack was not affected, and at high angles of attack the drag was reduced. The larger serrations (0.94 cm (0.37 in.)) adversely affected lift and drag.

The position of the serrations on the airfoil was a critical parameter. The most aft position tested, near the stagnation point at high angles of attack, proved to be the best location for increasing the lift. The performance was degraded with serrations on the airfoil chordline, a distance of only 0.95 cm (0.375 in.) forward of the best location.

Serration spacing or gap affected the model lift. Prong spacings of 0.75 cm (0.3 in.) and greater caused the highest maximum lift. Maximum lift was lower with serration gaps below 0.75 cm.

Flow visualization techniques showed that the serrations increased lift by generating vortices that trailed chordwise over the airfoil upper surface. The vortices brought higher energy air to the boundary layer delaying leading- and trailing-edge flow separation to higher angles of attack.

Protuberances on the upper surface of airfoils (ref. 4) are detrimental to lift and drag. Vortex generators on the upper surface (refs. 7 and 8) are capable of providing higher energy air to separated flow regions on airfoils. However, at high angles of attack they become ineffective if the flow separates upstream, enveloping the vortex generators. Properly designed vanes reported in reference 9 increased airfoil maximum lift 40 percent but caused a 20 percent drag rise at low angles of attack. The serrations used in this investigation had none of these difficulties when placed on the airfoil lower surface. Leading-edge serrations, therefore, have possible application for delaying flow separation on wings<sup>2</sup> and rotating blades as well as for the possible acoustic benefits mentioned in the introduction. The effect of serrations may be different for airfoils with stall mechanisms different from that of the model used in this study.

Ames Research Center  
National Aeronautics and Space Administration  
and  
U.S. Army Air Mobility R&D Laboratory  
Moffett Field, Calif. 94035, May 24, 1972

---

<sup>2</sup>This is also suggested in reference 10, but data are not presented.

## REFERENCES

1. Hickey, David H.: Some Developments In The Noise Reduction In Ducted Propellers and Fans. Conference on STOL Transport Aircraft Noise Certification, TR FAA-NO-69-1, Jan. 30, 1969, pp. 104-118.
2. Hersh, Alan S.; and Hayden, Richard E.: Aerodynamic Sound Radiation From Lifting Surfaces With and Without Leading-Edge Serrations. NASA CR-114370, 1971.
3. Hoerner, Sighard F.: Fluid-Dynamic Drag. S. F. Hoerner, Midland Park, N. J., 1965.
4. Jacobs, Eastman N.: Airfoil Section Characteristics as Affected by Protuberances. NACA Rep. 446, 1933.
5. Hopkins, Edward J.; Keating, Stephen J., Jr.; and Bandettini, Angelo: Photographic Evidence of Streamwise Arrays of Vortices in Boundary-Layer Flow. NASA TN D-328, 1960.
6. Görtler, H.: Dreidimensionale Instabilität der ebenen Staupunktströmung gegenüber wirbelartigen Störungen. 50 Jahre Grenzschichtforschung, H. Görtler and W. Tollmien, eds., V. F. Vieweg & Sohn (Braunschweig, Germany) 1955, pp. 304-314.
7. Bursnall, William J.: Experimental Investigation of the Effects of Vortex Generators on the Maximum Lift of a 6-Percent-Thick Symmetrical Circular-Arc Airfoil Section. NACA RM L52G24, 1952.
8. McFadden, Norman M.; Rathert, George A., Jr.; and Bray, Richard S.: The Effectiveness of Wing Vortex Generators in Improving the Maneuvering Characteristics of a Swept-Wing Airplane at Transonic Speeds. NACA TN 3523, 1955.
9. McCullough, George B.; Nitzberg, Gerald E.; and Kelly, John A.: Preliminary Investigation of the Delay of Turbulent Flow Separation by Means of Wedge-Shaped Bodies. NACA RM A50L12, 1951.
10. Lachmann, Gustav V.: Boundary Layer and Flow Control, Its Principles and Application, Vol. 2. Pergamon Press, New York, 1961, p. 1300.



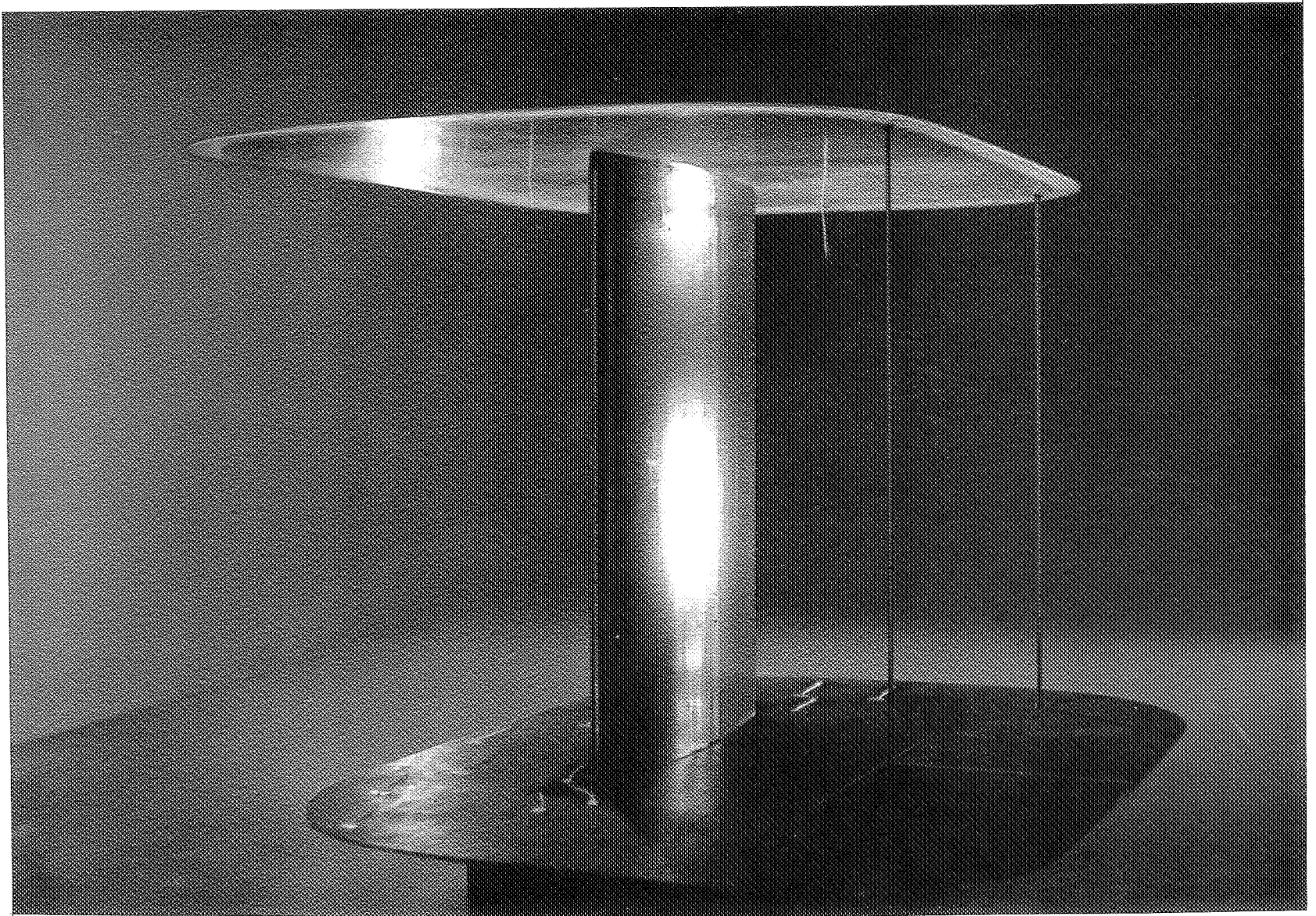
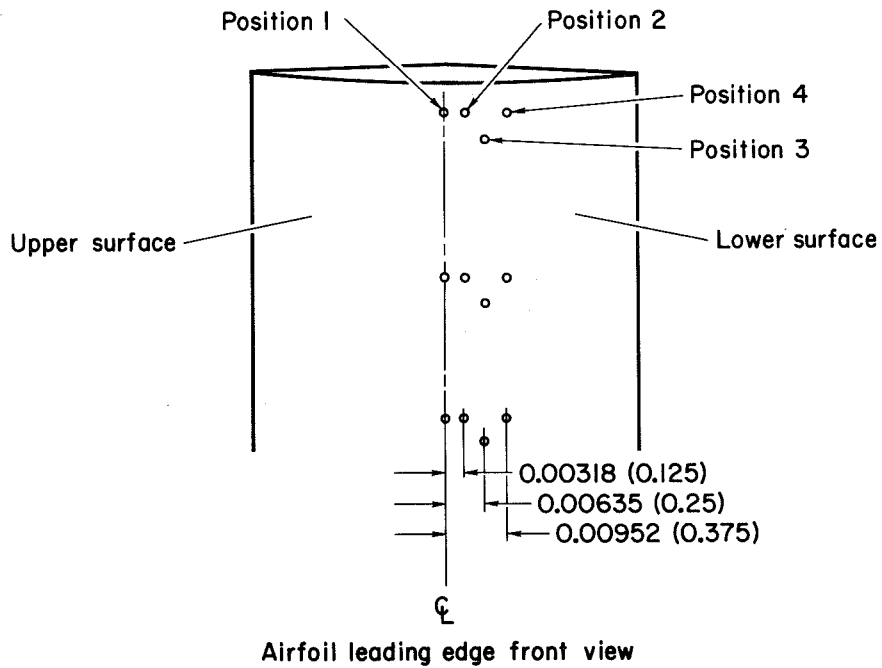
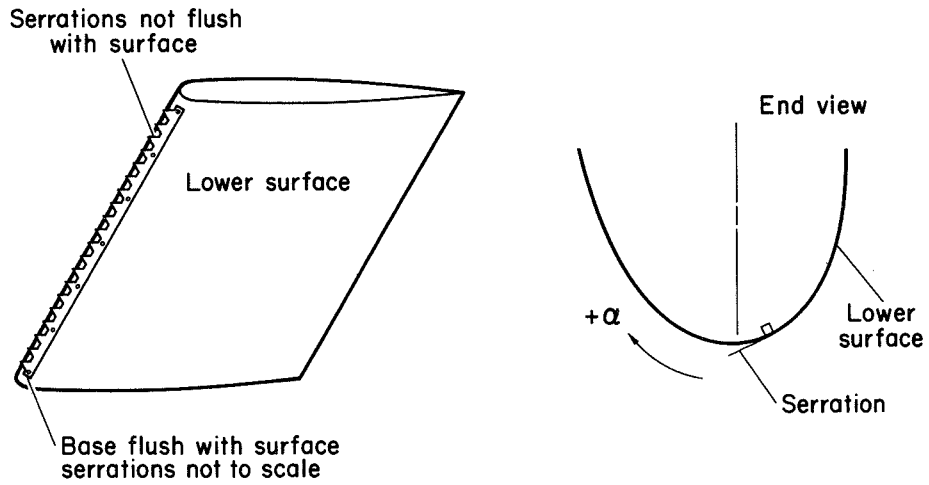


Figure 1. – The model in the Ames 7- by 10-foot wind tunnel.



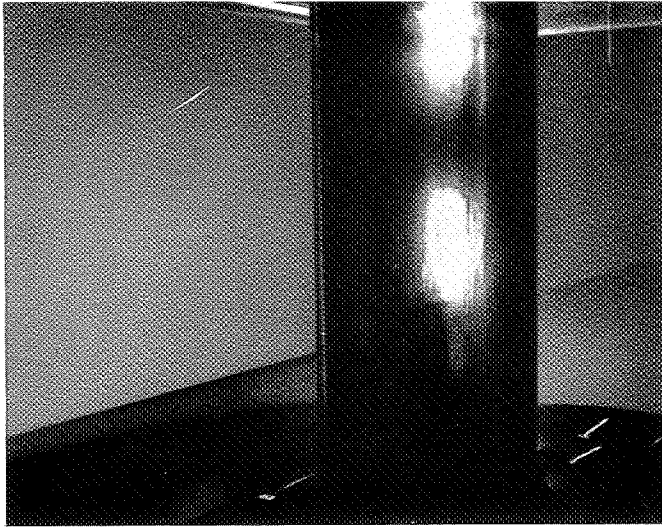




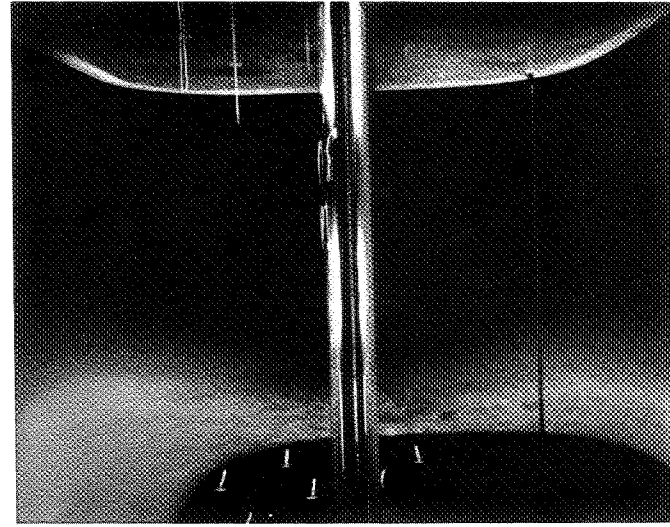
Note: all dimensions in meters (in.)

(c) Top – typical attachment of serration; bottom – chordwise locations of leading-edge serration attachment holes as measured along surface.

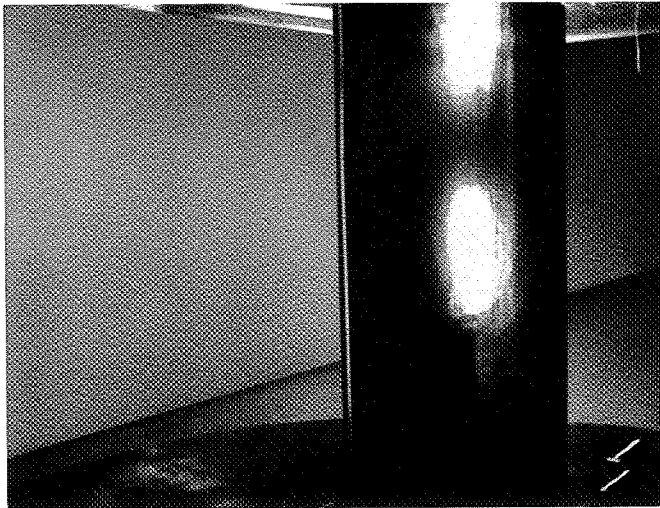
Figure 2.— Continued.



LE-5, position 3



LE-10, position 2



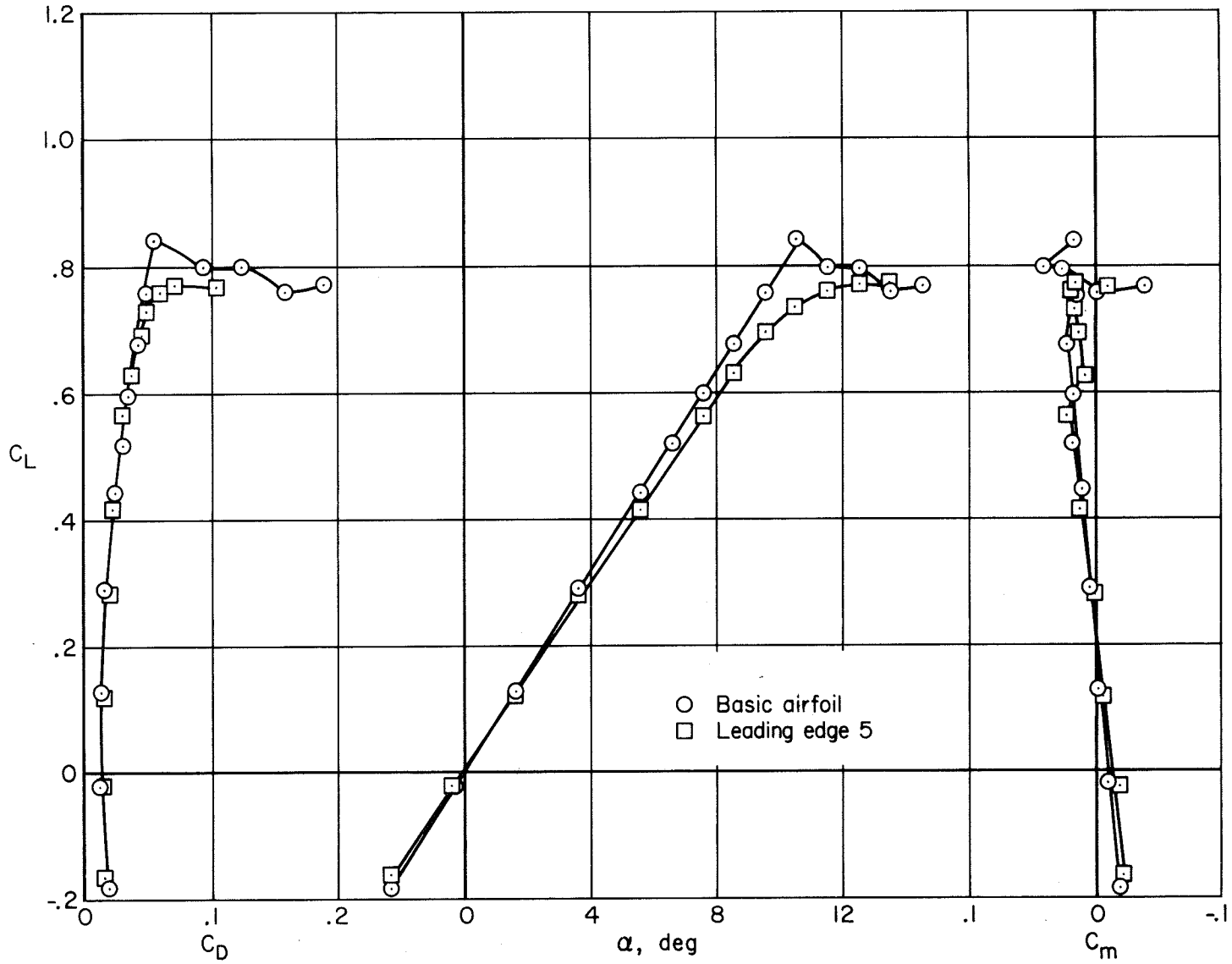
LE-11, position 3

(d) Photographs of model with typical serrations attached.

Figure 2.— Concluded.







(b) LE-5, position 3.

Figure 4.— Concluded.

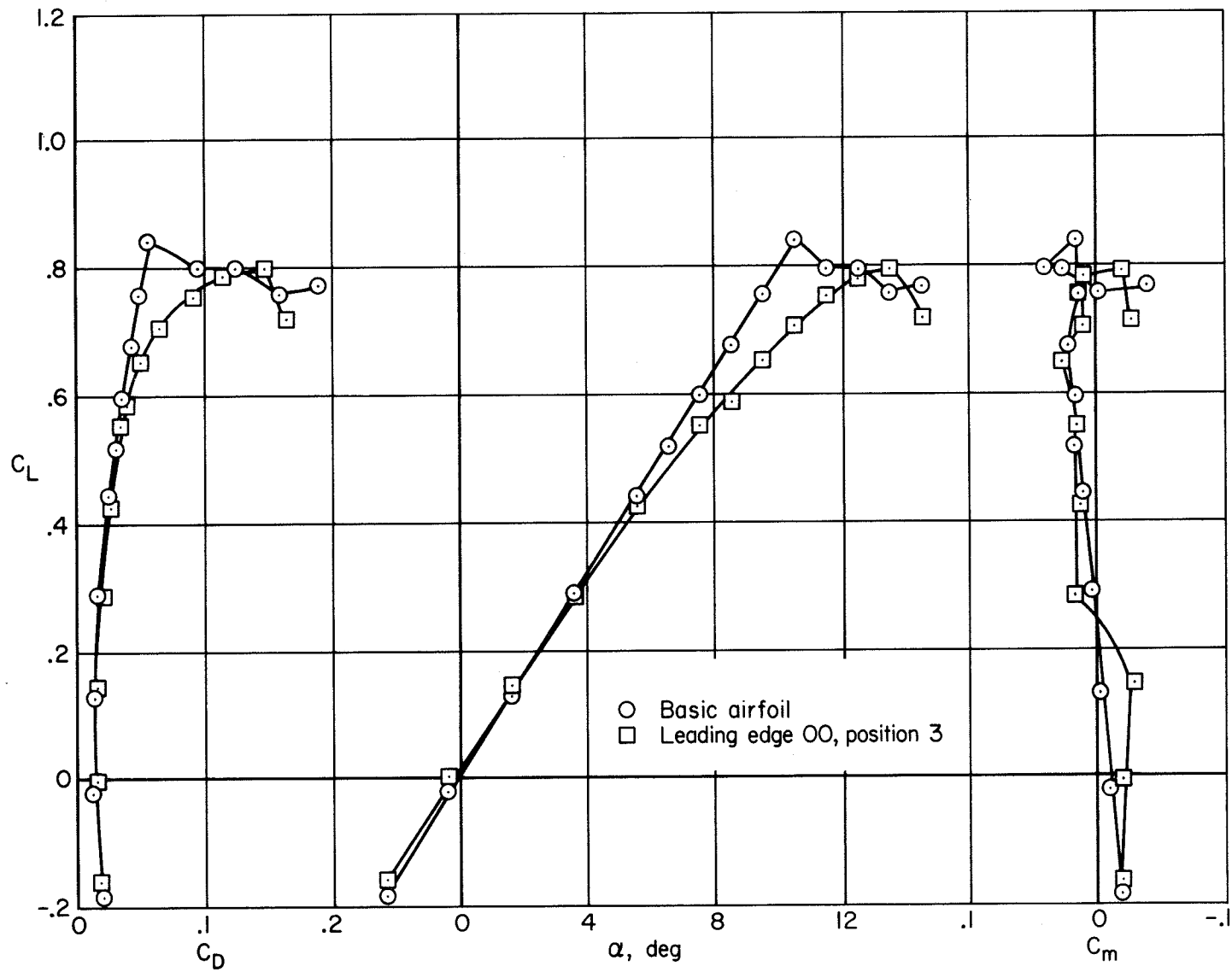
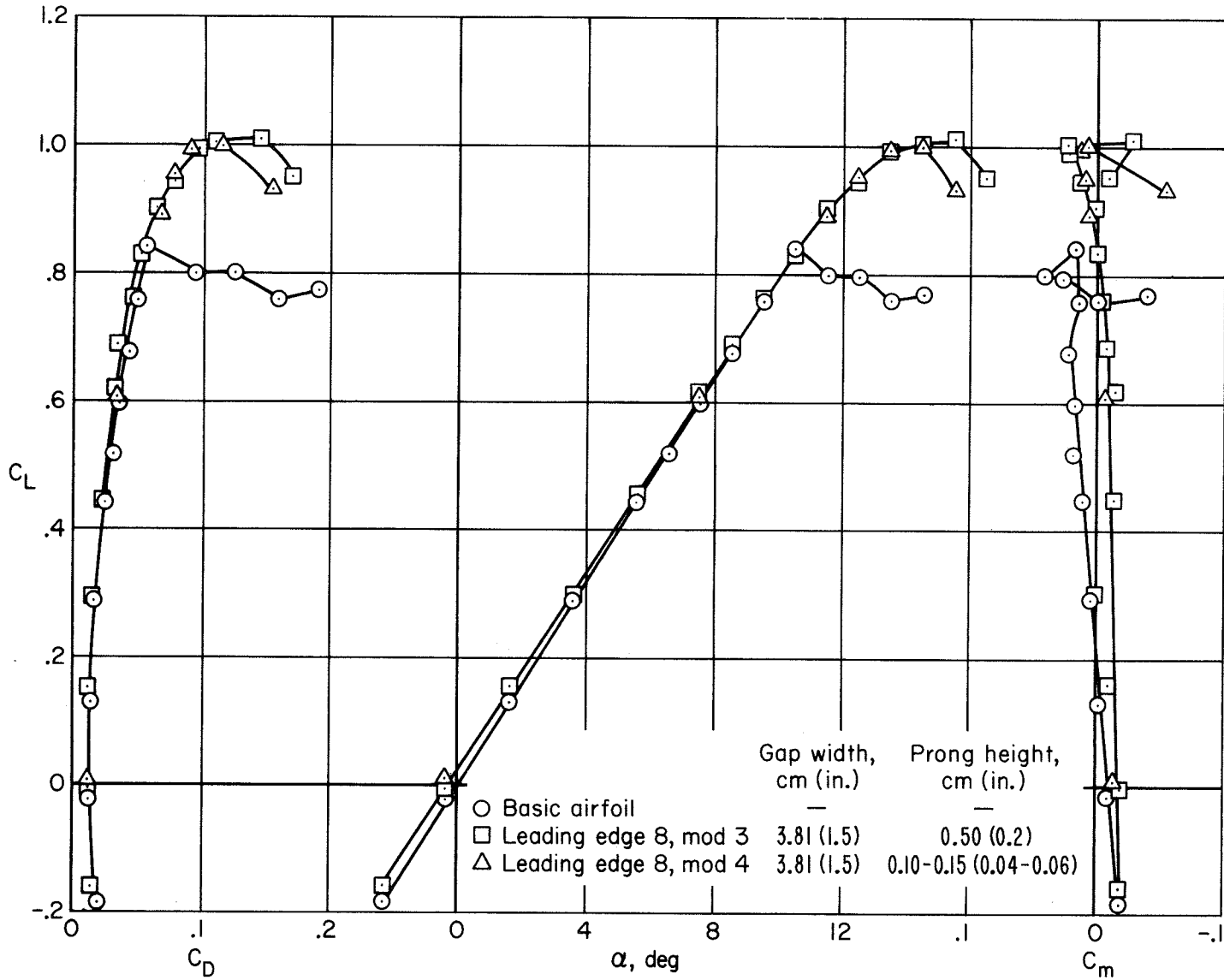


Figure 5.— Effect of leading-edge strip without serrations;  $q_\infty = 1197 \text{ N/m}^2$ .

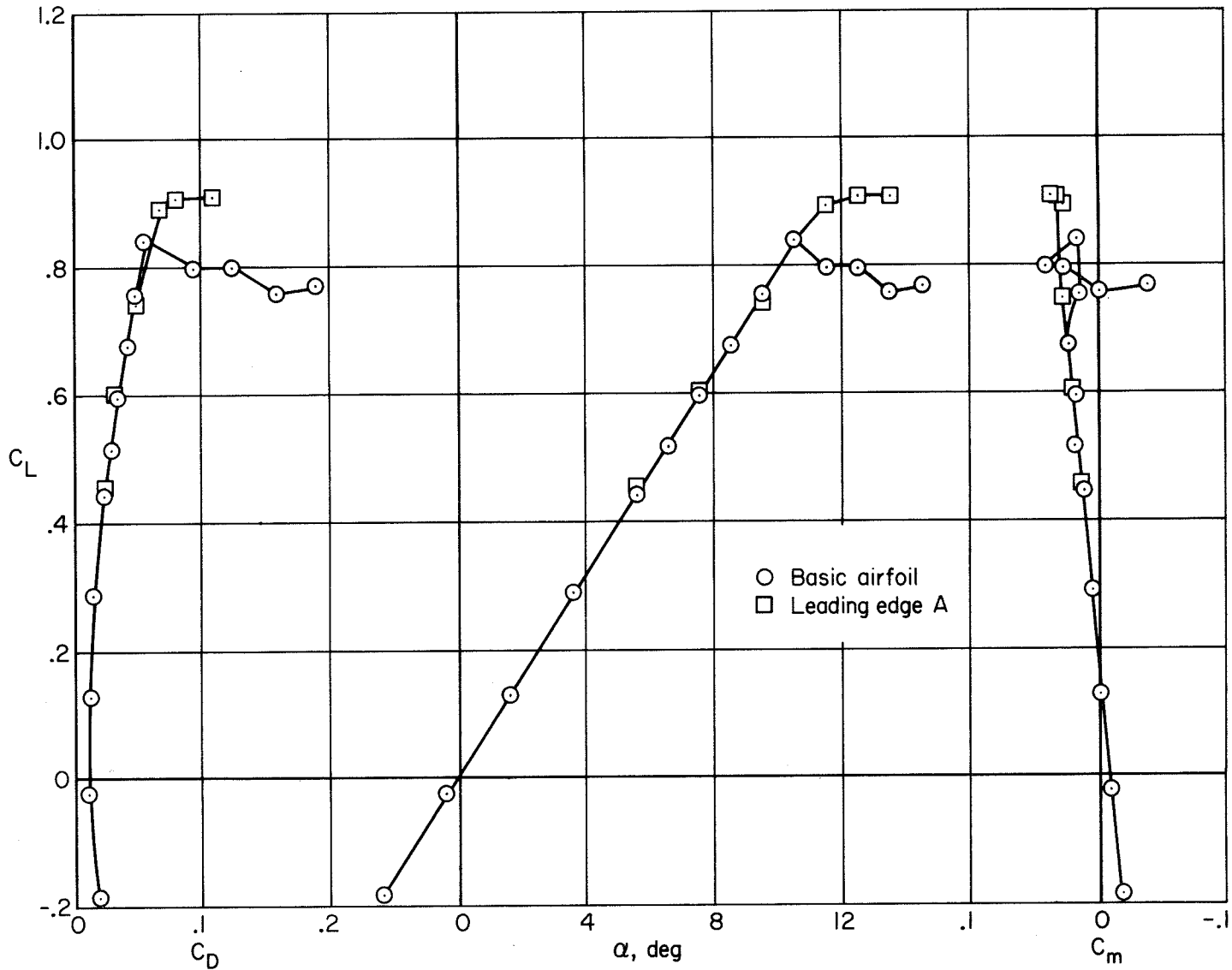






(b) Modifications 3 and 4.

Figure 7.— Concluded.



(a) LE-A, position 3.

Figure 8.— Effect of curved serration;  $q_\infty = 1197 \text{ N/m}^2$ .





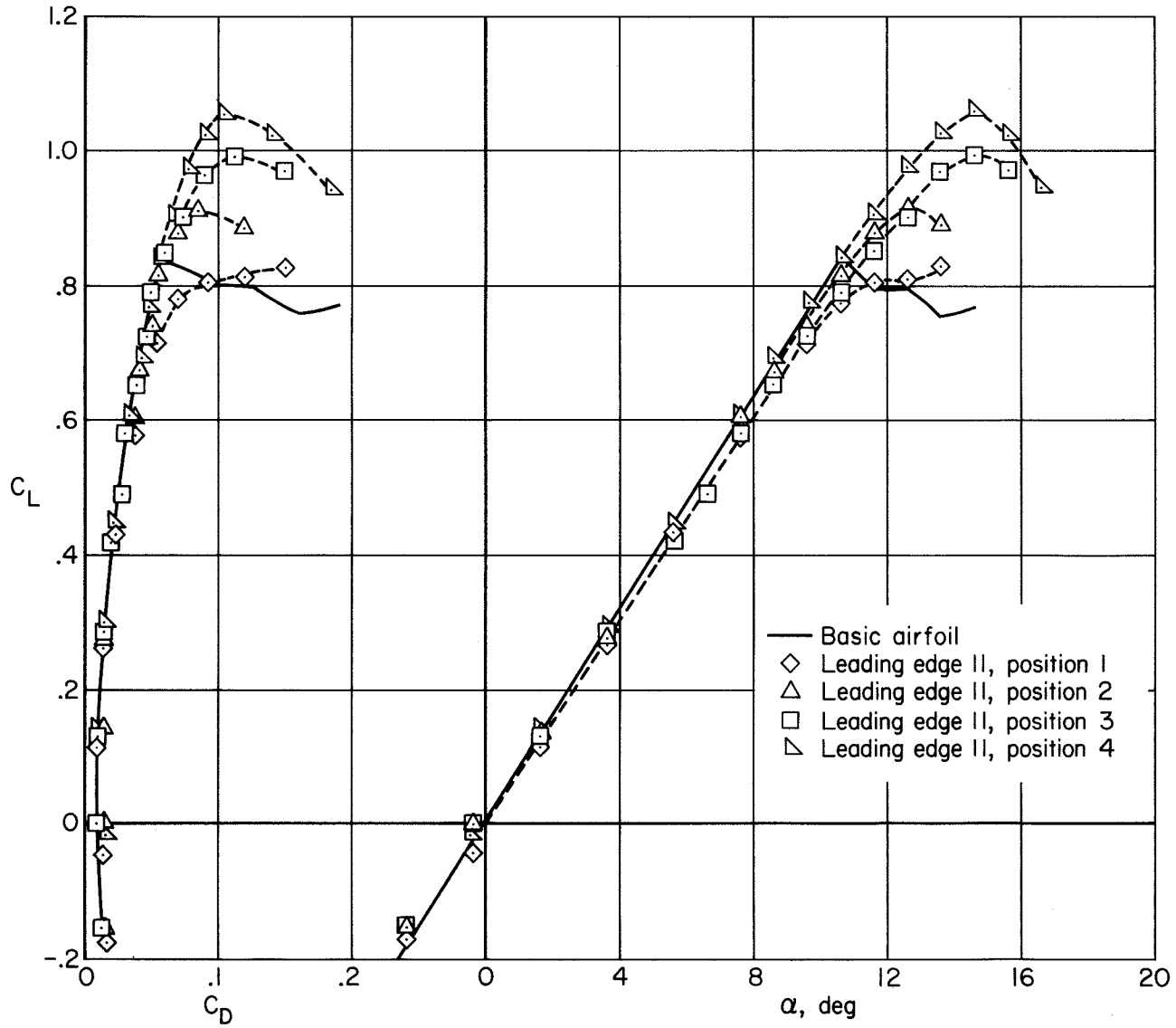


Figure 9.— Effect of serration location on airfoil;  $q_\infty = 1197 \text{ N/m}^2$ .

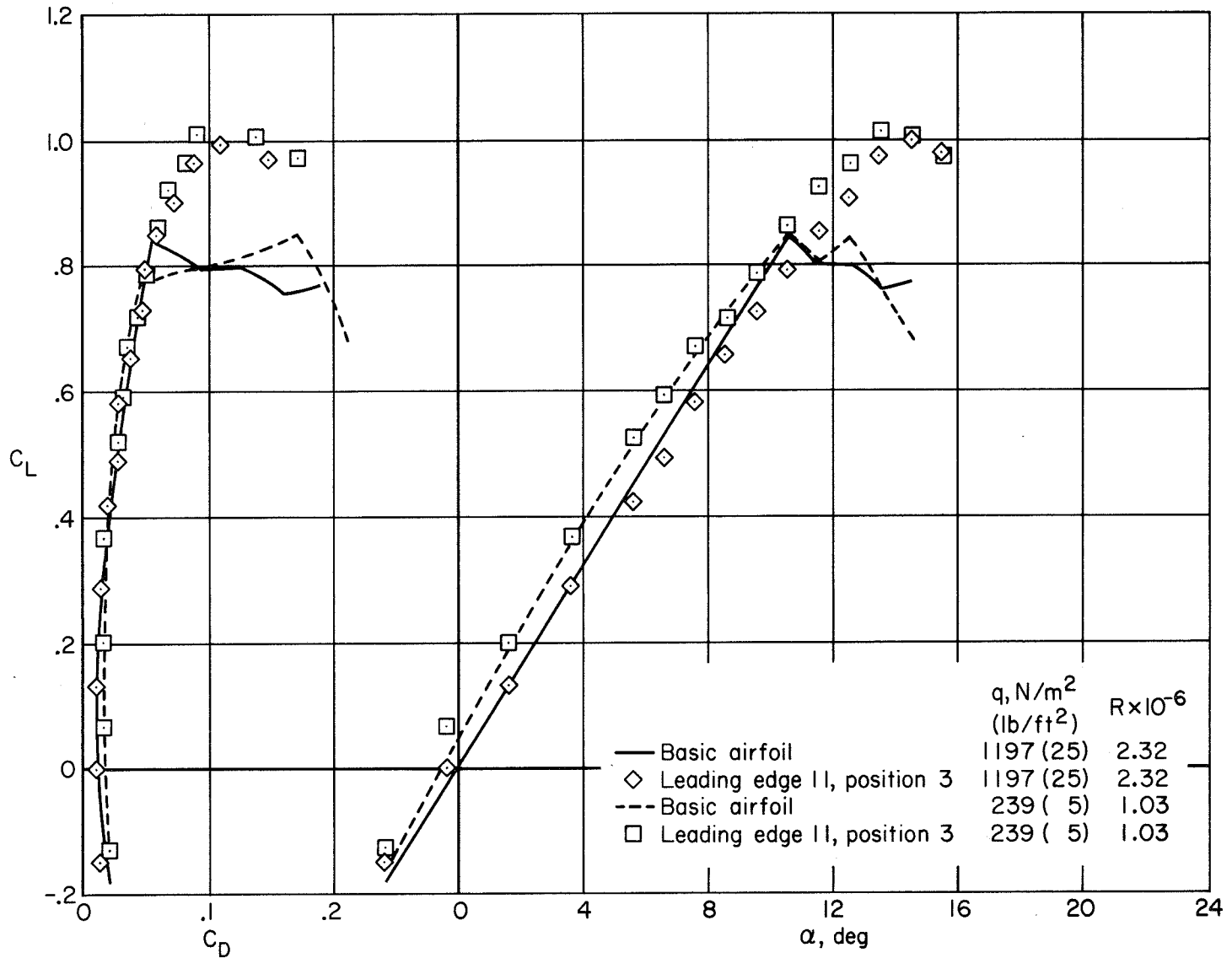
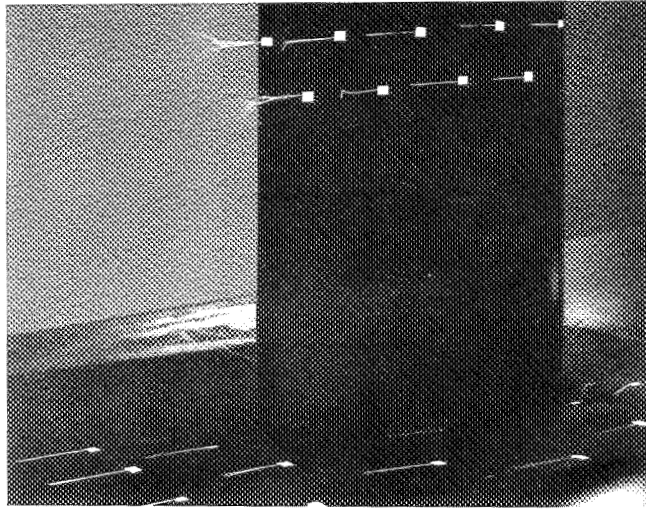
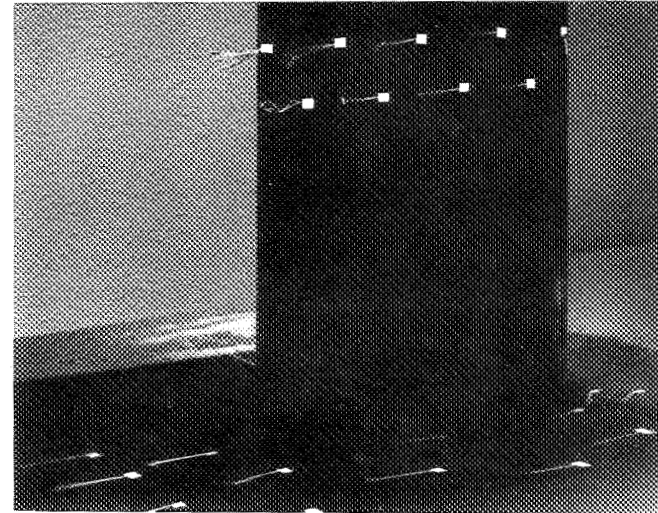
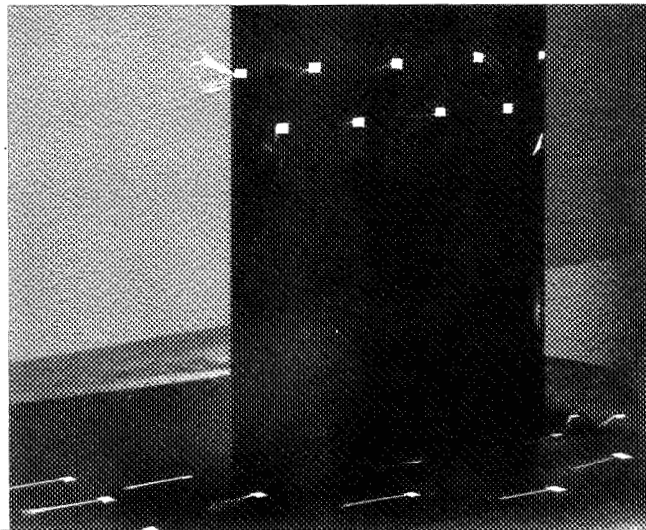


Figure 10.— Effect of Reynolds number.


 $\alpha = 11^\circ$ 

 $\alpha = 12^\circ$ 

 $\alpha = 13^\circ$ 

(a) Basic airfoil.

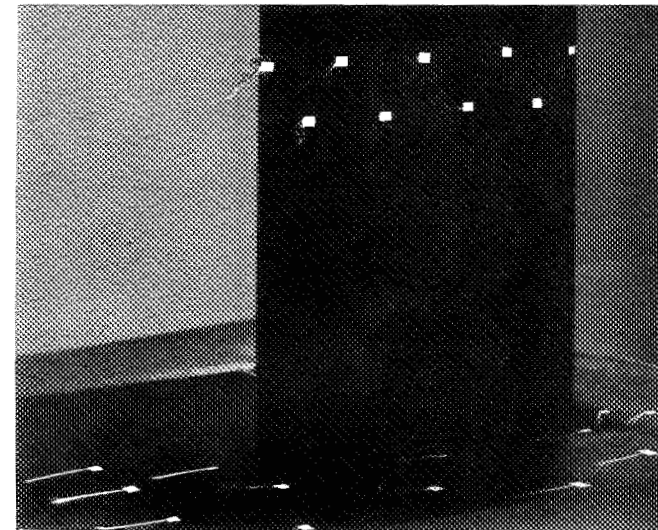
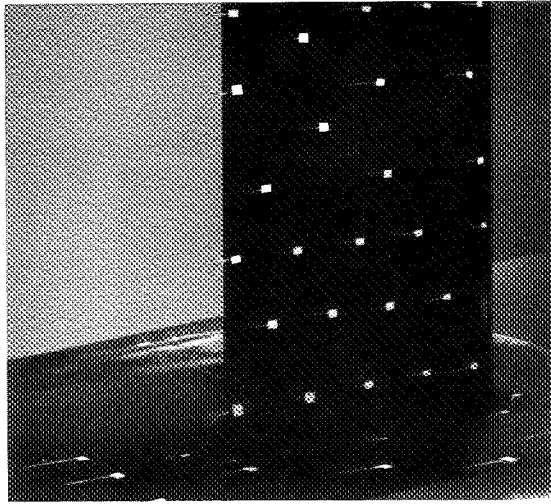
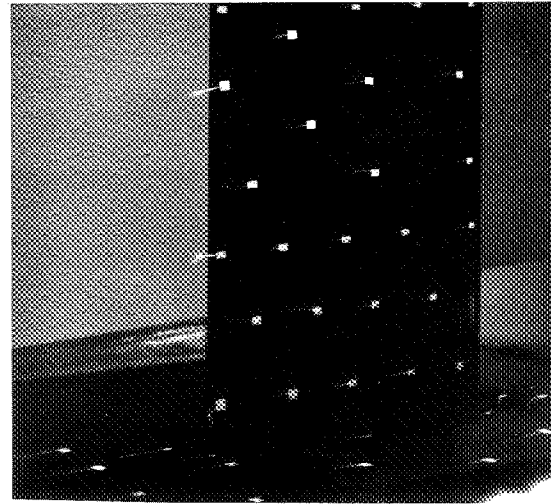

 $\alpha = 14^\circ$ 

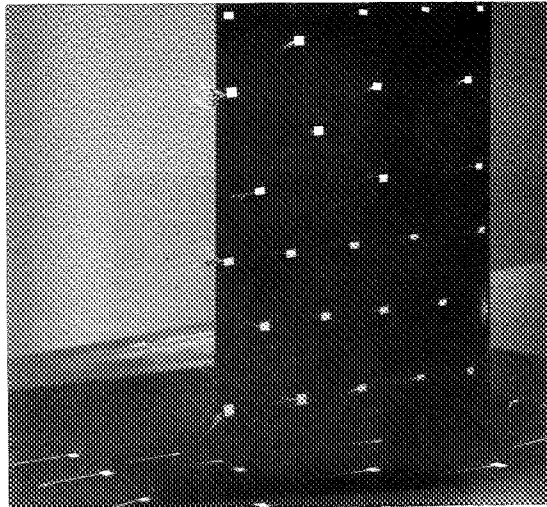
Figure 11.— Flow characteristics on the airfoil upper surface. All photographs except those in figure 11(c) are cut off at the upper end plate.



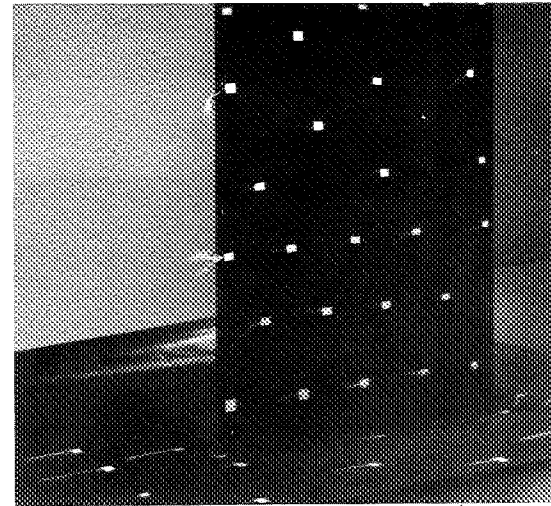
$\alpha = 11^\circ$



$\alpha = 12^\circ$



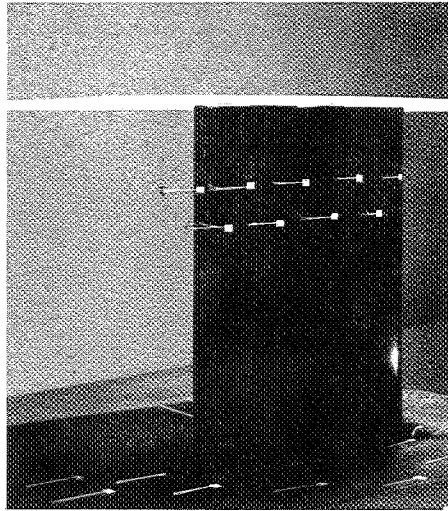
$\alpha = 13^\circ$



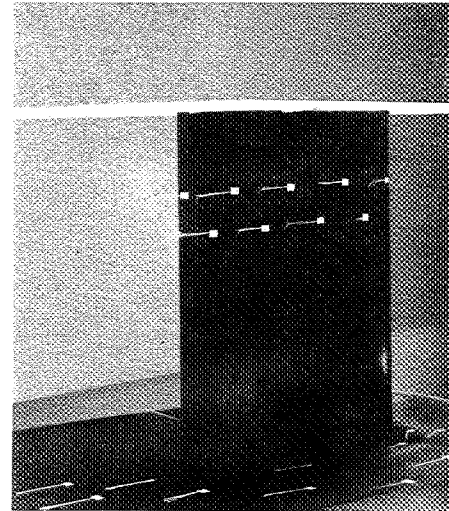
$\alpha = 14^\circ$

(b) Basic airfoil.

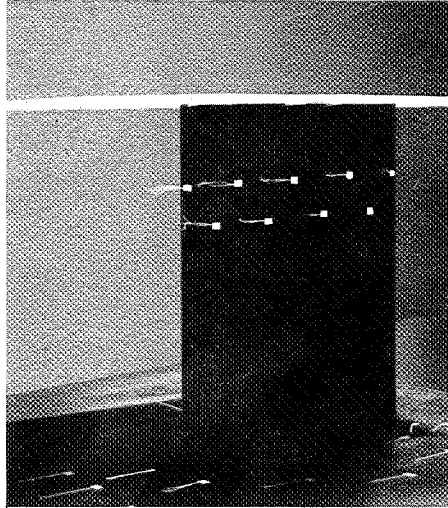
Figure 11.— Continued.



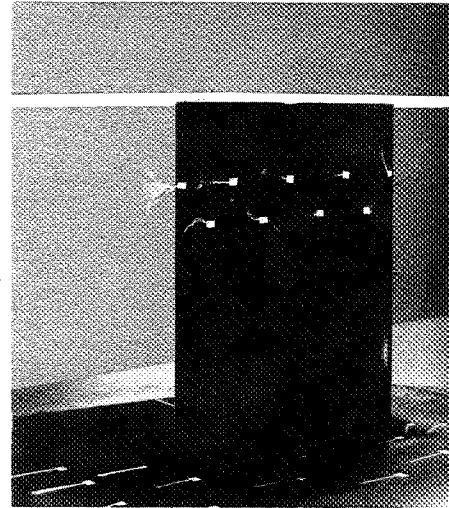
$\alpha = 9^\circ$



$\alpha = 10^\circ$



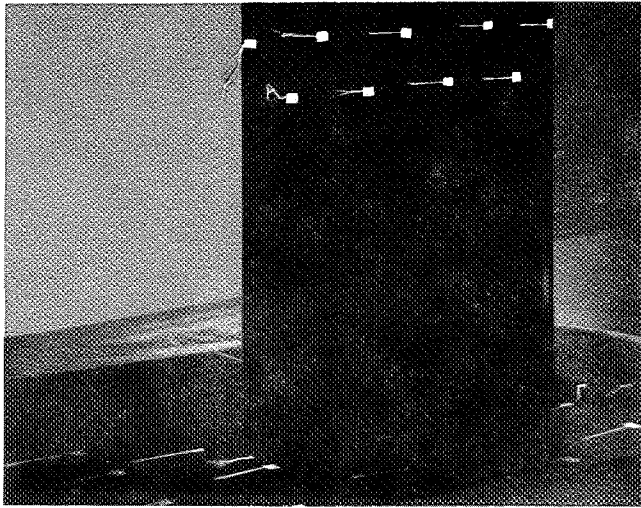
$\alpha = 11^\circ$



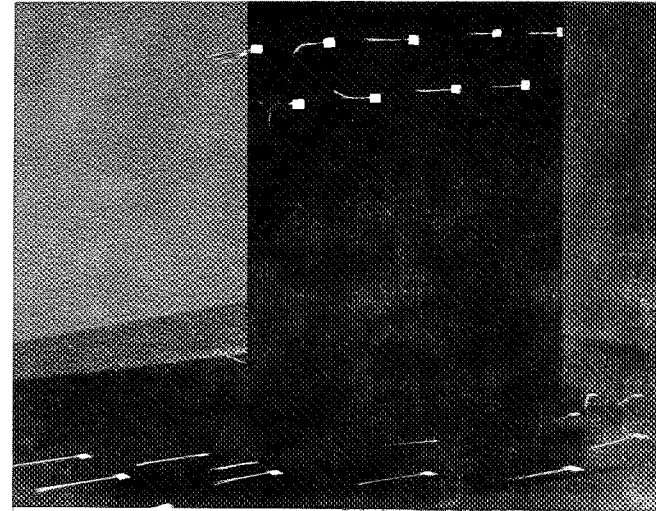
$\alpha = 12^\circ$

(c) LE-3, position 3.

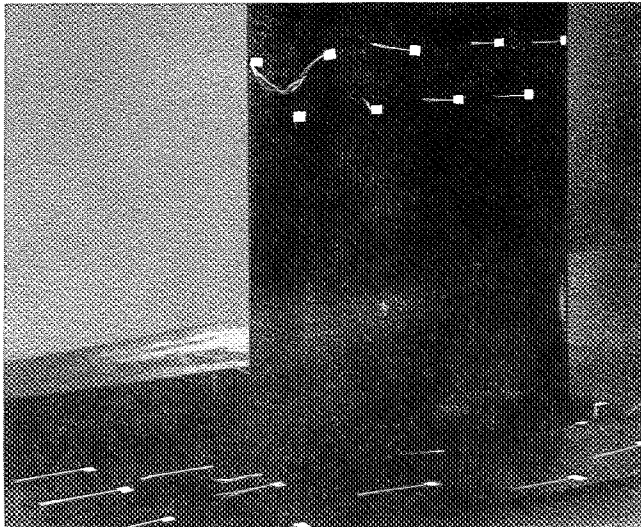
Figure 11.— Continued.



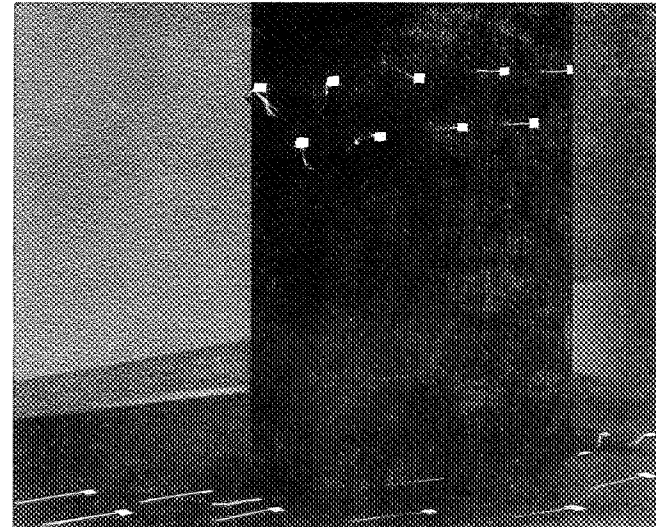
$\alpha = 12^\circ$



$\alpha = 13^\circ$



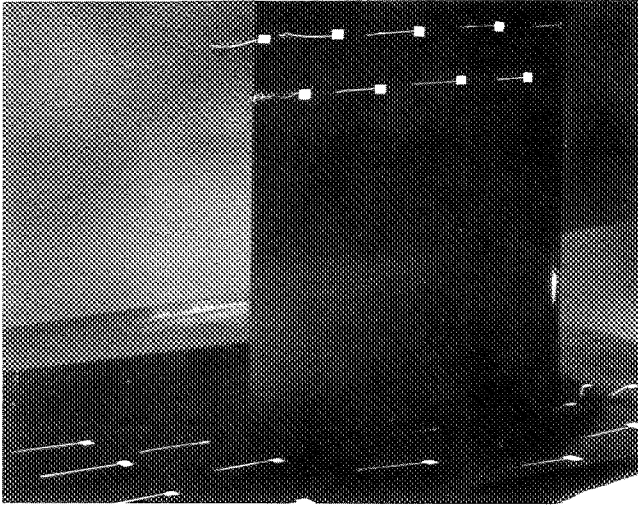
$\alpha = 14^\circ$



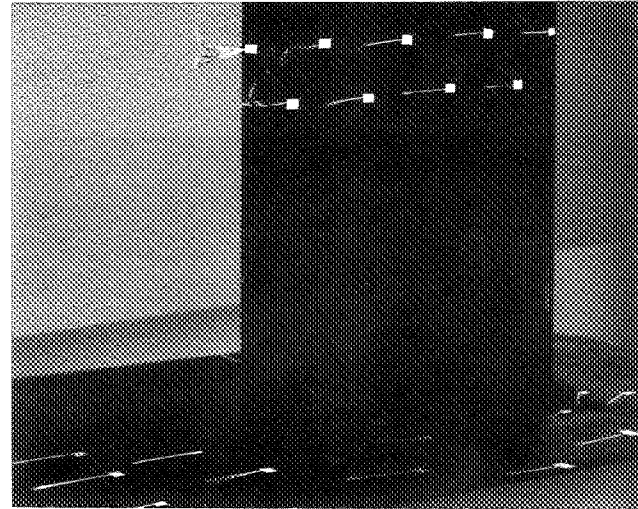
$\alpha = 15^\circ$

(d) LE-8, position 3.

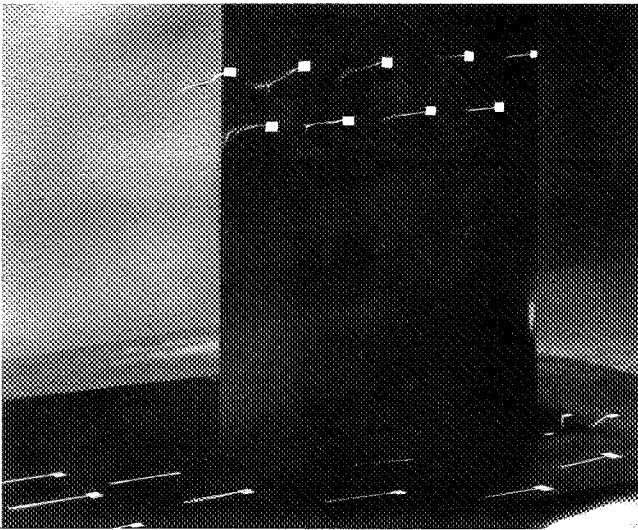
Figure 11.- Continued.



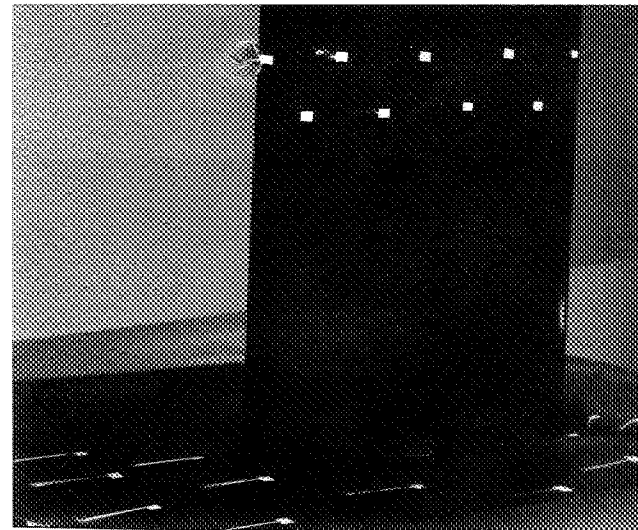
$\alpha = 12^\circ$



$\alpha = 13^\circ$



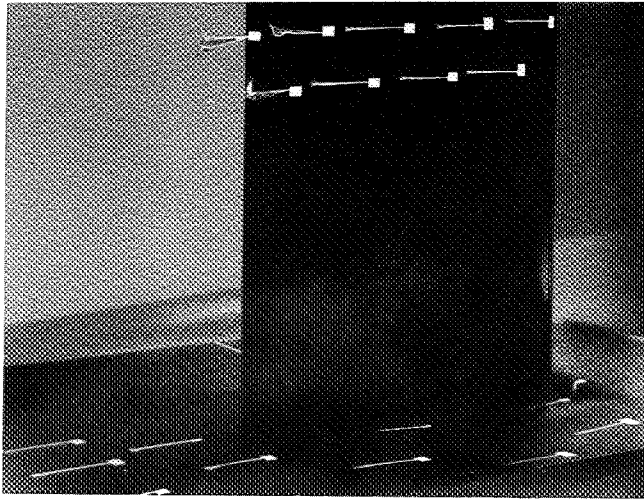
$\alpha = 14^\circ$



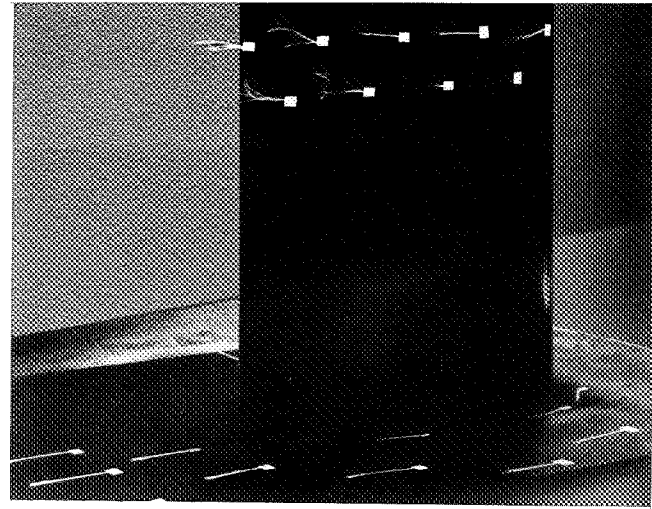
$\alpha = 15^\circ$

(e) LE-11, position 3.

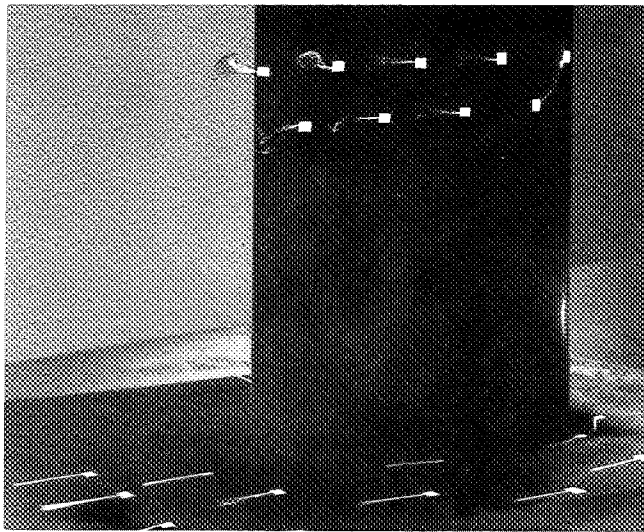
Figure 11.— Continued.



$\alpha = 12^\circ$



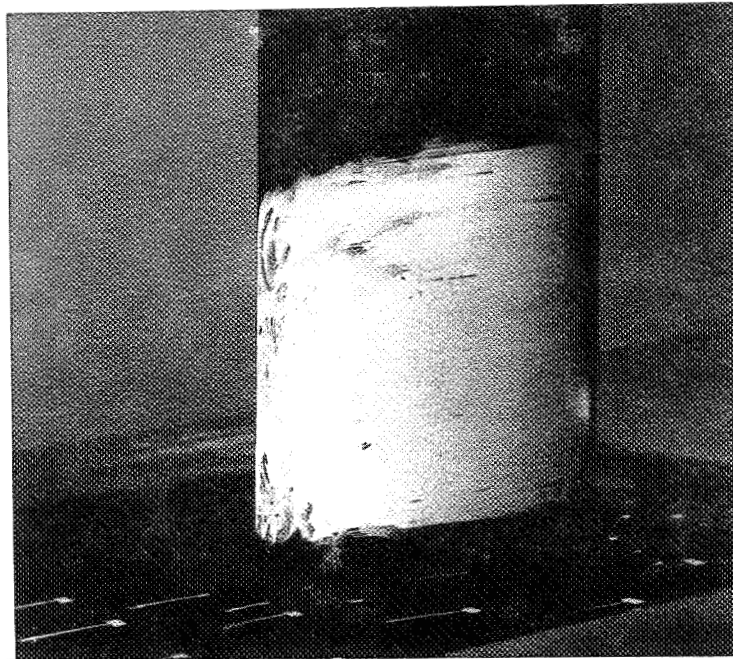
$\alpha = 13^\circ$



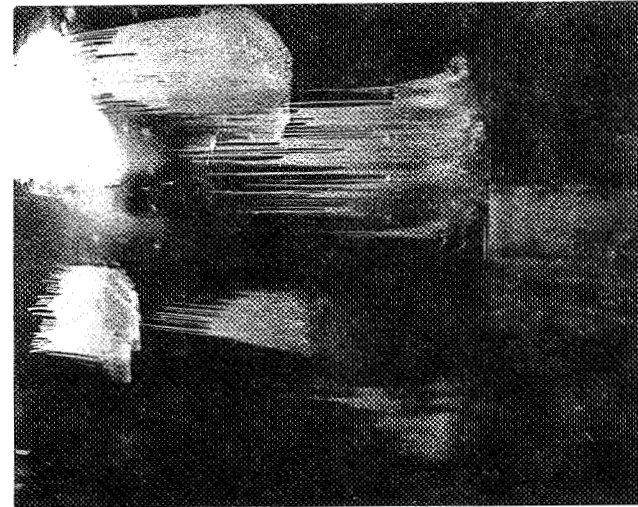
$\alpha = 14^\circ$

(f) LE-A, position 3.

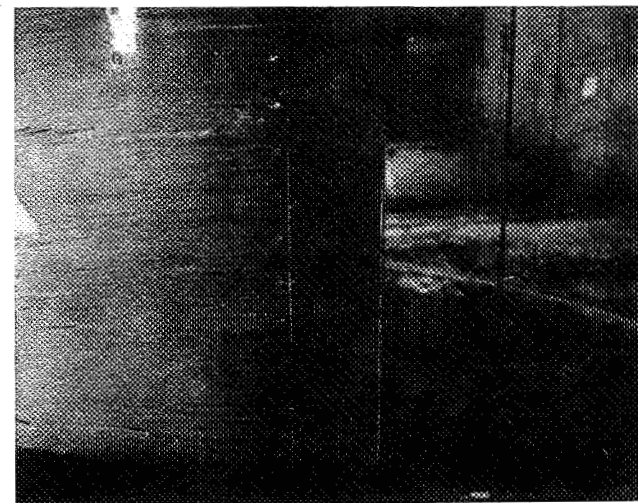
Figure 11.- Concluded.



LE-10, position 3,  $\alpha = 8^\circ$



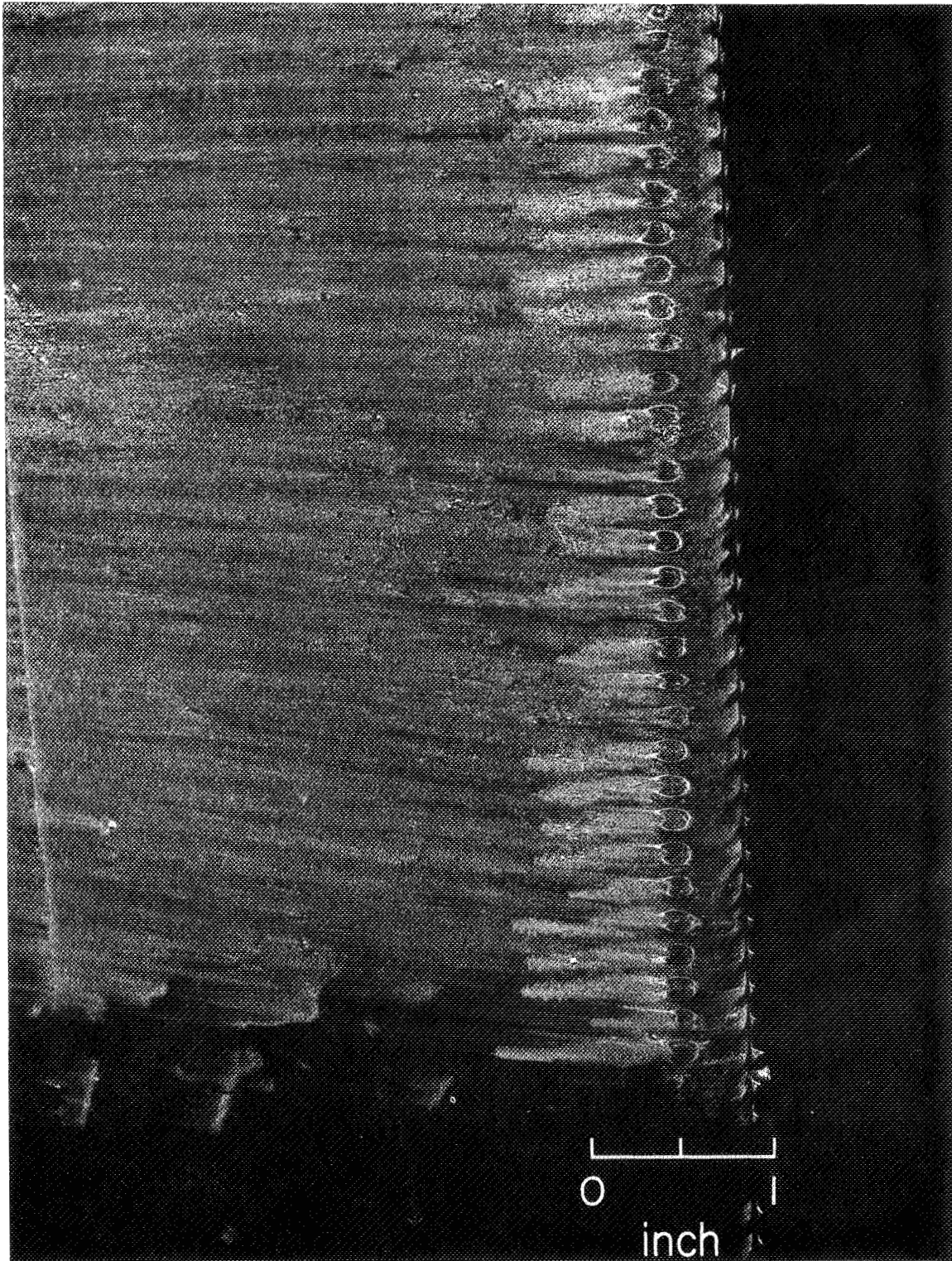
Basic airfoil,  $\alpha = 4^\circ$



LE-10, position 3,  $\alpha = 4^\circ$

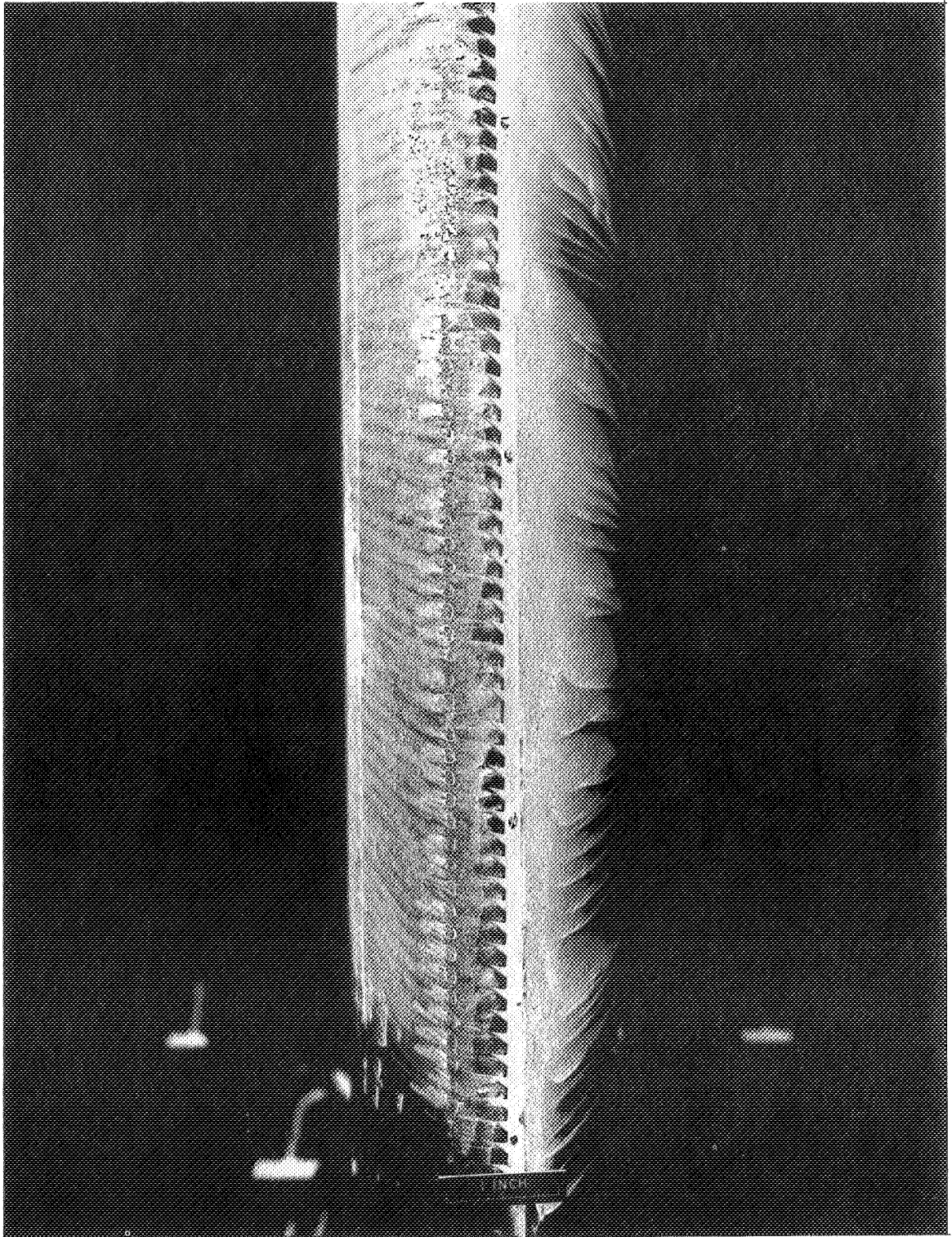
(a) Basic airfoil with and without LE-10, position 3.

Figure 12.— Photographs of oil flow,  $q_\infty = 1197 \text{ N/m}^2$ .



(b) Close-up of LE-10 and model upper surface, position 3,  $\alpha = 4^\circ$ .

Figure 12.— Continued.



(c) Close-up of LE-10, front view.

Figure 12.— Concluded.



POSTMASTER: If Undeliverable (Section 158  
Postal Manual) Do Not Return

*"The aeronautical and space activities of the United States shall be conducted so as to contribute . . . to the expansion of human knowledge of phenomena in the atmosphere and space. The Administration shall provide for the widest practicable and appropriate dissemination of information concerning its activities and the results thereof."*

— NATIONAL AERONAUTICS AND SPACE ACT OF 1958

## NASA SCIENTIFIC AND TECHNICAL PUBLICATIONS

**TECHNICAL REPORTS:** Scientific and technical information considered important, complete, and a lasting contribution to existing knowledge.

**TECHNICAL NOTES:** Information less broad in scope but nevertheless of importance as a contribution to existing knowledge.

**TECHNICAL MEMORANDUMS:** Information receiving limited distribution because of preliminary data, security classification, or other reasons.

**CONTRACTOR REPORTS:** Scientific and technical information generated under a NASA contract or grant and considered an important contribution to existing knowledge.

**TECHNICAL TRANSLATIONS:** Information published in a foreign language considered to merit NASA distribution in English.

**SPECIAL PUBLICATIONS:** Information derived from or of value to NASA activities. Publications include conference proceedings, monographs, data compilations, handbooks, sourcebooks, and special bibliographies.

**TECHNOLOGY UTILIZATION PUBLICATIONS:** Information on technology used by NASA that may be of particular interest in commercial and other non-aerospace applications. Publications include Tech Briefs, Technology Utilization Reports and Technology Surveys.

*Details on the availability of these publications may be obtained from:*

**SCIENTIFIC AND TECHNICAL INFORMATION OFFICE  
NATIONAL AERONAUTICS AND SPACE ADMINISTRATION  
Washington, D.C. 20546**